

UCLA

UCLA Previously Published Works

Title

Detection and Segmentation Of Shape-Coded Particles Via Hough Transforms and Snake Active Contours

Permalink

<https://escholarship.org/uc/item/0n54c6xm>

Authors

Brown, Jason

Arnheim, Alyssa

Bertozzi, Andrea L

et al.

Publication Date

2024-03-19

DOI

10.1109/ssiai59505.2024.10508613

Peer reviewed

DETECTION AND SEGMENTATION OF SHAPE-CODED PARTICLES VIA HOUGH TRANSFORMS AND SNAKE ACTIVE CONTOURS

Jason Brown^{1,4*}, Alyssa Arnheim^{2*†}, Andrea L. Bertozzi^{1,3,4*}, Dino Di Carlo^{2,3,4}

¹ Department of Mathematics, ² Department of Bioengineering, ³ Department of Mechanical and Aerospace Engineering and ⁴ California NanoSystems Institute, University of California, Los Angeles, Los Angeles, CA 90095, USA.

ABSTRACT

Shape-coded particles enable multiplexed diagnostics, offering advantages such as reduced reagent usage, enhanced accuracy through swarm-sensing, and decreased reliance on spectral barcoding. These particles exhibit the capability to stabilize nanoliter aqueous droplets in the inner annular region, facilitating signal amplification while maintaining independent particle-based reactions. The resulting endpoint fluorescence of these droplets correlates with the biomarker concentration in the patient sample, providing valuable information for disease diagnosis. Each distinct shape can be assigned to different patients or biomarkers, enabling the collection of more comprehensive information in each diagnostic test. In order to automate the process of measuring fluorescence, it is necessary to develop methods for detecting the particles and segmenting them while differentiating the shapes. In this paper, we use the circle Hough Transform, Merlin-Farber Algorithm, and snake active contours for distinguishing and segmenting circle and square particles. Without using any deep learning, these methods can successfully identify and segment the particles under various conditions.

Index Terms— Circle Hough Transform, Merlin-Farber Algorithm, Snake Active Contours, Detection, Segmentation

1. INTRODUCTION

To tackle the issue of mass parallel medical testing, special microscopic annular particles have been developed [1]. These particles serve as the solid surface for a particle-based immunoassay, capable of trapping and detecting biomarkers of interest. Prior work using these particles reported the detection of a heart failure biomarker across clinically relevant ranges [2]. High fluorescence in the internal cavity of the particle indicates the presence of the biomarker. However, accurate results from this biomarker test rely on accurate identification of the particles across a variety of lighting conditions.

For commercial use of such particles at scale, there is need for a reliable, autonomous system that detects and segments the particles in images. A recent work uses deep learning methods for this problem on a similar dataset with ten different particle shapes with approximately 102-152 samples per shape [3]. A natural limitation of deep learning is that there must be sufficiently large and varied data to train on as well as time and energy dedicated towards annotating the dataset. Deep learning is well-known to produce highly variable results when training with one dataset and applied to an independent dataset, especially if the unknown data is collected under differing conditions. We propose an alternative approach, for circle and square particles, with similar performance, that can be calibrated on a small number of images and is adaptable to many different laboratory environments. The proposed method is also constructed in a way that would allow for a priori error estimates for each identified shape, because it is based on the local geometry of particles.

Our work is, in part, inspired by earlier work on blood cell segmentation. For example, [4] uses a k-means clustering on the pixel values to separate the blood cells from the background followed by the watershed segmentation method. Another method [5] involves the Canny edge detection method and shape geometry. For dispersion control of circular particles [6], the circle Hough Transform has been used and compared with deep methods as well as the ellipse and line segment detector method [7].

Unlike some of the blood cell datasets, the particles in our dataset are largely transparent (see Figure 1), therefore requiring edge based methods. We combine the Canny Edge Detection [8] method for both the circle Hough Transform [9] and Merlin-Farber Algorithm [10]. After detection, we employ snake active contours [11, 12] to segment the squares. Python code for our method is available on Github¹.

*Supported by Simons Math + X Investigator Award number 510776

†Supported by the NSF PATHS-UP Engineering Research Center 1648451

¹<https://github.com/jasbrown96/ParticleDetectionSeg>

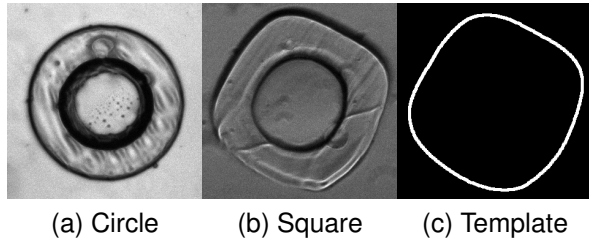


Fig. 1. Cropped images of (a) a circle particle, (b) a square particle and (c) the square template

2. DATA

The dataset consists of images with size (2048x2048) taken using a Nikon Eclipse Ti2 microscope. The particles were photographed within the well of a 24-well plate. Images were collected at 4x magnification and all bright field images were captured using phase microscopy to accentuate the features of the particles.

3. METHODS

The process for detecting and segmenting the circle and square particles is shown in Figure 2 and outlined here:

- 1. Canny Edge Detector:** Applied to the image.
- 2. Circle Hough Transform:** Applied to the edges using the known radius of the circle particles.
- 3. Merlin-Farber Algorithm:** Applied to detect squares. (Algorithm 1).
- 4. Post Process Peaks:** First, apply non-max suppression and enforce that centroids be separated by a distance of the radius of the particles. Second, if a particle is detected as both a square and circle, it is classified as a circle since circle Hough transform has higher confidence.
- 5. Segment:** For the squares, initialize a circular snake about the centroid with a radius large enough to exclude the inner annular region. Use a positive edge attraction and adaptive balloon force to ensure that the area of the snake is within tolerance of the square.

3.1. Particle Detection

Template matching is a method to detect specific shapes in images. Given some image $I(x, y)$ and a template $T(x_2, y_2)$, the most simple and straightforward way to proceed with the template matching involves a cross-correlation of the template with the image

$$(T \star I)(x, y) = \sum_{(x_t, y_t) \in T} T(x_t, y_t) \cdot I(x_t + x, y_t + y).$$

When the template aligns with the desired shape in the image, centered at some (x^*, y^*) , the value of $(T \star I)(x^*, y^*)$ will be

Algorithm 1 Merlin-Farber Algorithm

INPUT: The edges, $E(x, y)$, and a template $T(x_2, y_2)$.

OUTPUT: The accumulator array $A(x, y)$.

Rotate the template by 180° .

Initialize empty, padded accumulator array A .

FOR each (i, j) such that $E(i, j) = 1$

Update accumulator array: $A(i - \frac{x_2}{2} : i + \frac{x_2}{2}, j - \frac{y_2}{2}, j + \frac{y_2}{2}) += T$

Remove padding from A

large[13]. This approach is computationally time-consuming, does not benefit from sparsity in the images, and may require a large search space for shape, size, and orientation.

For our images, we instead use the well-known circle Hough transform[9] for the circular particles and the Merlin-Farber Algorithm[10] for the square particles, which benefits from the sparsity introduced via the Canny edge detector. The Merlin-Farber Algorithm is a generalized Hough transform and although there are other versions of the generalized Hough transform, this algorithm is sufficient for our needs. For the square particles, we have a fixed size template that matches the boundary of the shape from the Canny edge detector applied to the microscopy images, shown in (c) of Figure 1. The templates have 90° rotational symmetry, greatly simplifying the search space since fewer orientations need to be checked.

To describe the Merlin-Farber Algorithm for the squares, we consider the edges of the image

$$E(x, y) = \begin{cases} 1 & (x, y) \text{ is an edge} \\ 0 & \text{otherwise} \end{cases}$$

and a binary edge template $T(x, y)$ defined similarly. Let (a, b) be a reference point for the template, usually the center of the template. For each edge in the template, (x^*, y^*) , we can construct a vector pointing from the edge to the reference location $r_{(x^*, y^*)} = (a - x^*, b - y^*)$. The collection of these vectors can be used in a similar fashion to the circle Hough Transform, where a given edge pixel can now vote in the accumulator matrix towards a potential reference point.

An efficient way to implement this process is to rotate the template image by 180° and then use this rotated template as a mask and add to the accumulator array wherever an edge pixel is detected. This process is outlined in (Algorithm 1).

If a particle is detected as both a square and circle, we would classify the particle as a circle due to stronger uniformity in the circular particles.

3.2. Segmentation

Once the particles have been detected and the centroids located, the next step is to segment the particles. For the circles, this is quite straightforward as the radius is also determined during the detection process. Implicitly, a segmentation is found by simply selecting all of the pixels that are a radius's

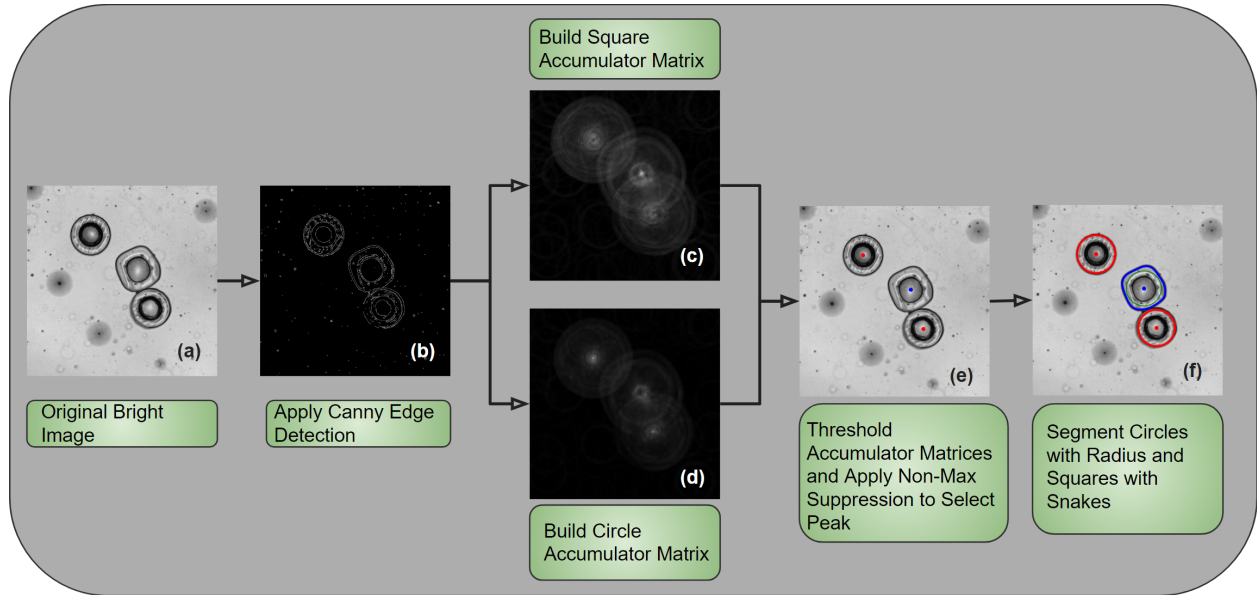


Fig. 2. The flowchart for the procedure. (a) Shows the original bright image before any processing has been done. (b) Shows the edges detected by the Canny edge detector. (c) Shows the accumulator matrix from Merlin-Farber Algorithm. Note the brightest points in each image correspond to the detected centroids for the shapes. (d) Shows the circle accumulator matrix from the circle Hough transform. (e) After thresholding the respective matrices and applying non-max suppression, we see the detected centroids. The blue dot corresponds to the square centroid and the red dots correspond to the circle centroids. (f) Shows the segmentation results. The circles are segmented from the knowledge of their radii and the square is segmented with a snake. The initial curve for the snake is shown by the green line and the final contour is shown in blue.

distance away from the located centroid. For the square particles, more work is required. Although the template matching process does give insight into the boundary of the particle, there is less uniformity in the square particles and the orientations may not line up exactly. For these reasons, we look for a method that offers local fine-tuning. We consider the variational segmentation method known as snakes, which are active, edge-based contours that iterate until convergence[11]. Snakes evolve an initial curve to minimize external and internal energies.

Snakes, as introduced by Kass[11], will contract and converge on edges. However, this contraction requires the initial curve for the snake to be outside of the particle. This means convergence will be difficult for overlapping or adjacent particles that might introduce additional edges to converge to. To solve this problem, we use balloon snakes [12]. A balloon force on the snake is an additional energy term that dictates whether the curve should expand or contract. With this additional energy term, we can choose initializations for the snake from within the particle and allow the snake to converge from within, assured that there is minimal noise present. The initialization for the snake is chosen to be a circle with radius large enough to exclude the inner annuli but small enough to stay within the particle. Due to the uniformity of the particles, this is easily achieved. The next challenge is in balancing the hyperparameters for the energy in the snake. Notably, we are concerned with balloon forces that are too large, pushing the snake outside the particle, or too small, allowing for conver-

gence on the inner annuli or noise. To solve this, we fix the internal and external energy parameters and use an adaptive search to find an ideal balloon force for each of the particles that guarantees the area enclosed by the snake is near the area of the square particles.

4. EXPERIMENTS AND RESULTS

We choose 15 images that contain combinations of square and circular particles under various conditions to tune hyperparameters and use 5 additional images for testing. For the Canny edge detector, we use a sigma value of 0, low threshold of 100, and high threshold of 150. For the circle Hough Transform, we use the Sci-Kit image library and a threshold of 0.25. We search over circles with radius between 120 and 130 pixels. In order to use the Merlin-Farber Algorithm for the square particles, we need to generate various templates that we expect to match with. We use the template seen in (c) of Figure 1 as the guideline and then nine rotated variants of the template with rotation spacing of 10° , utilizing the 90° rotational symmetry in the squares. More templates would improve accuracy but increase computation time. With these 10 references, we use a threshold of 60 to indicate a detection of a square. In the non-max suppression, we select the greatest peaks and enforce a distance of 150 pixels between peaks, roughly correlating to the radius of the particles. The snakes for the square particles are initialized as circles centered on the detected centroid with a radius of 110 pixels. We

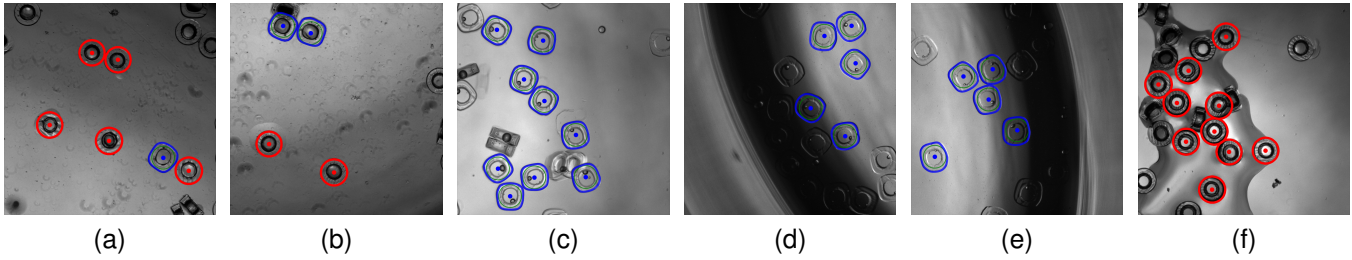


Fig. 3. Results from the method applied to various images of particle wells. Circle centroids and boundaries are marked in red. Square centroids and boundaries are marked in blue with the green curve showing the initialization for the snake. Particles near or on the edge of an image are filtered out of the dataset prior to the image analysis.

use $\alpha = 0.03$, $\beta = 10$, $\gamma = 0.001$, $w_{line} = 0$, $w_{edge} = 1.5$ as the snake parameters and begin the balloon force search with $\delta = 0.003$. The upper and lower limits for the allowed snake area is 58000 and 54500 square pixels respectively.

We note that in these experiments, particles near or on the boundary were not included for detection and segmentation purposes. In the 20 image dataset, we count that there are 62 reasonably identifiable square particles and 49 reasonably identifiable circle particles. Our method correctly detects and segments 59 of the square particles and 40 of the circle particles. There are no false positives, which is ideal for medical testing. The false negatives all occurred on darkened regions of the images, likely leading to a failure in edge detection.

Figure 3 shows an overlay of the detected centroids and segmentations for 6 notable images that were chosen to showcase various conditions. In (a) and (b), the images contain a mixture of the circles and squares demonstrating differentiation between types. Images (c), (d), and (e) showcase square detection, the harder task, in the presence of overlapping particles, miscellaneous artifacts, and varying light conditions. Here we note that particles on the edge of the imaging well are often covered in darkness and thus are very difficult to detect due to low contrast. In (f), we show detection of circle particles in the presence of liquid on the imaging tray. Although some of the particles are not detected, a large amount of them are despite the noise in the image.

5. CONCLUSION

The problem of detecting and segmenting the mixed particles under various lighting conditions is quite challenging. This presentation of classical techniques for solving the problem not only automates the process of detecting and segmenting the particles, but is done in a fashion that is interpretable and allows for simple calibration of parameters for the instrument used, which is often not possible with deep learning techniques. Further work would consider additional particle morphologies to increase the scalability of the method, as well as using other generalized Hough transforms beyond the Merlin-Farber Algorithm.

6. REFERENCES

- [1] G. Destgeer, M. Ouyang, C.-Y. Wu, and D. Di Carlo, "Fabrication of 3d concentric amphiphilic microparticles to form uniform nanoliter reaction volumes for amplified affinity assays," *Lab Chip*, vol. 20, pp. 3503–3514, 2020.
- [2] V. Shah, X. Yang, A. Arnheim, S. Udani, Y. Luo, M. Ouyang, G. Destgeer, O. Garner, H. Koydemir, A. Ozcan, and D. Di Carlo, "Amphiphilic particle-stabilized nanoliter droplet reactors with a multimodal portable reader for distributive biomarker quantification," *ACS Nano*, vol. 17, pp. 19952–19960, 2023.
- [3] G. Destgeer, M. Akif Sahin, L. van den Eijnden, and C. Bhiri, "Deep learning based recognition of shape-coded microparticles," *Frontiers in Lab on a Chip Technologies*, vol. 2, pp. 1248265, 2023.
- [4] Congcong Zhang, Xiaoyan Xiao, Xiaomei Li, Ying-Jie Chen, Wu Zhen, Jun Chang, Chengyun Zheng, and Zhi Liu, "White blood cell segmentation by color-space-based k-means clustering," *Sensors*, vol. 14, no. 9, pp. 16128–16147, 2014.
- [5] Fatimah Al-Hafiz, Shiroq Al-Megren, and Heba Kurdi, "Red blood cell segmentation by thresholding and canny detector," *Procedia Computer Science*, vol. 141, pp. 327–334, 2018.
- [6] Pavel V. Gulyaev, "Application of the hough transform to dispersion control of overlapping particles and their agglomerates," *Devices and Methods of Measurements*, vol. 14, pp. 199–206, 2023.
- [7] V. Pătrăucean, P. Gurdjos, and R. Grompone Von Gioi, "A parameterless line segment and elliptical arc detector with enhanced ellipse fitting," in *Computer Vision—ECCV 2012: 12th European Conference on Computer Vision, Florence, Italy, October 7–13, 2012, Proceedings, Part II 12*. Springer, 2012, pp. 572–585.
- [8] John Canny, "A computational approach to edge detection," *IEEE Transactions on Pattern Analysis and Machine Intelligence*, vol. PAMI-8, no. 6, pp. 679–698, 1986.
- [9] Richard O Duda and Peter E Hart, "Use of the hough transformation to detect lines and curves in pictures," *Communications of the ACM*, vol. 15, no. 1, pp. 11–15, 1972.
- [10] Philip M Merlin and David J. Farber, "A parallel mechanism for detecting curves in pictures," *IEEE Transactions on Computers*, vol. 100, no. 1, pp. 96–98, 1975.
- [11] Michael Kass, Andrew Witkin, and Demetri Terzopoulos, "Snakes: Active contour models," *International journal of computer vision*, vol. 1, no. 4, pp. 321–331, 1988.
- [12] Laurent D Cohen, "On active contour models and balloons," *CVGIP: Image understanding*, vol. 53, no. 2, pp. 211–218, 1991.
- [13] Azriel Rosenfeld, "Picture processing by computer," *ACM Computing Surveys (CSUR)*, vol. 1, no. 3, pp. 147–176, 1969.